TUJNAS
ISSN-Print: 2073-0764
ISSN-Online: 2959-4340

Thamar University Journal of
Natural & Applied Sciences
(TUJNAS)

Journal website:
www.tu.edu.ye/journals/index.php/TUJNAS/index

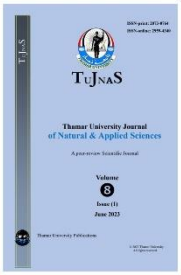

ORIGINAL ARTICLE

Synthesis, Structural, Optical and Electrical Properties of Pure and Doped NiO Nanostructures Prepared via The Co-precipitation Method

Enas Ali Ahmed Alahsab, Abdullah A. A. Ahmed*, A. M. Abdulwahab

Affliations:
Department of Physics, Faculty of Applied Science, Thamar University, Dhamar 87246, Yemen.

Corresponding Author:
Abdullah A. A. Ahmed, emails: abdullah2803@gmail.com or abdullah2803@tu.edu.ye

Received: May 12, 2023,

Revised Date: Jun 6, 2023,

Accepted Date: Jun 12, 2023,

Online Date: Jun 13, 2023

Published: Jun 13, 2023

DOI:
https://doi.org/10.59167/tujnas.v8i1.1491

Abstract

Here, we report the synthesized high purity NiO nanostructures using simple and inexpensive chemical route. NiO NPs and (Cu, Zn) single and dual doped NiO NPs prepared by co-precipitation technique and annealed at 350 ℃ for 2 hours. Structural properties of prepared samples were investigated by X-ray diffraction (XRD). The optical characterizations and electrical conductivity were characterized by UV-vis spectrophotometer and I-V measurement. The crystallite size for dual doped NiO samples was 7.9 ± 0.9 nm compared to pure NiO, which had 9.52 nm. These results are consistent with the ionic radii of the doped metals. The obtained values of the band gap energy increased from 3 eV for pure sample to higher values (3.14 ± 0.06 eV) for doped samples due to the quantum confinement effect. These results agreed with the DC conductivity of samples. The ionic conductivity σ_{ionic} was developed with dual doping. The characterization of the doped samples makes them good candidates for photoelectronic applications.

Keywords

Nickel oxide nanostructures; Dual doping; Band gap energy; Electrical properties

1. Introduction

Nickel oxide (NiO) is a green crystalline solid material with ferromagnetic properties and a Neel temperature of 523 K. NiO has unique electrical, magnetic, and optical properties that make it the primary subject of numerous applications. NiO is a material with extreme chemical stability. Due to its low cost and excellent ion storage property, it has become an interesting research material [1]. NiO NPs is a p-type conductivity due to its wide energy band gap from 3.6 eV to 4.0 eV [2, 3]. There are several methods to synthesis of NiO NPs such as electro deposition (ED), hydrothermal method [4] Sol-gel, thermal decomposition and Chemical precipitation [1, 5, 6]. NiO nanoparticles can be used in various applications like photocatalytic, battery, electrochromic, chemical sensing applications [7-9] and gas sensor application [4].

The doped NiO NPs lead to improvement of physical properties for various applications. K Varunkumar *et al.,* reported on Cu doped NiO NPs prepared by co-precipitation and studied optical and thermal stability, the bandgap increased from 3.32 to 3.37 eV at 8 (wt %) and showed exhibit good thermal stability [10]. K. Varunkumar *et al.,* studied morphology of the pure NiO and Cu doped NiO NPs at different calcination temperatures 350 °C, 450 °C and 550 °C that revealed spherical shaped particles for pure NiO and Cu doped NiO samples calcined at 350 °C while changes were observed for other calcination temperatures [11]. Zn doped NiO nanoparticles were synthesized by co-precipitation method at calcination temperature of 550˚C and the optical band gap was found at 3.26 eV [12]. Solvothermal synthesis of pure and Zn doped NiO nanocluster electrocatalysts resulted in higher conductivity with lower internal resistance (Rs) of 10.36 Ω for the above optimized electrocatalyst [9]. Recently, Zn-doped NiO thin films were synthesized for highly sensitive and selective ammonia sensors [13].

In the present study, pure, single and dual (Cu and Zn) doped NiO nanoparticles were synthesized by co-precipitation method and structure, optical and electrical properties of the prepared samples were reported.

2. Experimental Details

2.1 Materials

Nickel nitrate hexahydrate $Ni(NO_3)_2.6H_2O$ (Fluka, ≥ 98%), copper nitrate trihydrate $Cu(NO_3)_2.3H_2O$ (Scharlau, extra pure), zinc nitrate hexahydrate $Zn(NO_3)_2.6H_2O$ (Fluka. ≥ 98%) and sodium hydroxide (95%). The solvent used for all mentioned chemicals was distilled water.

2.2 Synthesis of pure NiO Nanostructures

1 M nickel nitrate solution was prepared by dissolving 14.54 g in 50 ml distilled water with constant stirring for 20 min. 0.1 M NaOH was added dropwise to the nickel nitrate solution to adjust the pH to 10 and stirred at room temperature for 3 h until a light green colored solution was obtained. The final solution was kept in an airtight container for one day to obtain the precipitate, which was centrifuged at 4000 rpm for 15 minutes and then washed several times with distilled water. The collected precipitate was dried at 80 ℃ for 15 h and then ground into fine powder with mortar and pestle. Finally, the powder was annealed at 350 ℃ for 2 h to obtain a pure NiO nanostructure.

2.3 Synthesis of Cu-Zn dual doped NiO Nanostructures

Copper nitrate and zinc nitrate solutions were prepared separately in 5 concentrations (0.025, 0.05, 0.075 and 0.1 M). The mixing of different solutions was clarified in Table 1 to obtained single and dual doped NiO according to the formula $Ni_{0.9}(Cu_{1-x}Zn_x)_{0.1}O$, where x = 0, 0.25, 0.5, 0.75 and 1. As presented in Table 1, there were two single doped NiO samples at x = 0 (Cu only) and one (Zn only) and 3 dual doped NiO samples (at x = 0.25, 0.5 and 0.75). x value indicated to the increase of Zn doped percentage in NiO from 0 to 0.1 as x value increased from 0 to 0.01 and decreasing of Cu doped percentage in the same time from 0.1 to 0.

0.9 M of nickel nitrate solution was prepared in 75 ml of distilled water under constant stirring for 20 min and labeled as solution (A). For sample prepared at x = 0.25, 0.025 M zinc nitrate and 0.075 M copper nitrate solutions were prepared separately in 75 ml of distilled water under constant stirring for 20 min and labeled as solution (B) and (C), respectively. Solutions A, B and C were mixed under constant stirring for further hour at RT. The pH value of the mixed solutions was adjust to 10 by addition of 0.1 M NaOH drop by drop under constant stirrer for 3 h at RT. The light green solution was obtained and kept in an airtight container for a day to collect the precipitate. The precipitate was filtered and centrifuged at 4000 rpm for 15 min and then washed with distilled water several times. The final precipitate was dried in oven for 15 h at 80℃. Then it was grind using mortar and pestle to get fine powder and finally, powder was annealed at 350 ℃ for 2 h to obtain $Ni_{0.9}Cu_{0.075}Zn_{0.025}O$ nanostructure. The other samples were prepared by repeating of the above procedures for all x values according to arranged concentrations in Table 1.

2.4 Characterizations

The structural properties of prepared samples have investigated using the X-ray diffraction (XRD) technique (XD-2 X-ray diffractometer using CuKα (λ = 1.54 Å) at 36 kV and 20 mA, China) in Yemeni Geological Survey and Minerals Resources Board (YGSMRB).

The absorbance and transmittance spectra of samples were measured using a UV–VISIBLE spectrophotometer (SPECORD 200) at room temperature in the wavelength range of (190–1100 nm). The diluted hydrochloric (HCl) acid was used as a solvent for prepared samples to measure the absorbance and transmittance spectra. The powder of all prepared samples was pressed into pellet forms with a thickness of about 1 mm and a diameter of 13 mm using a Carver hydraulic press machine. These pellets were used to measure the DC electrical conductivity at room temperature.

Table 1: Experimental details for preparation of single and dual doped NiO nanostructures.

Samples	Concentrations in (M)			Doping type	x value
	Nickel nitrate (doping %)	Copper nitrate (doping %)	Zinc nitrate (doping %)		
$Ni_{0.9}Cu_{0.1}O$	0.9	0.1 (10%)	- (0%)	Single	x = 0
$Ni_{0.9}Cu_{0.075}Zn_{0.025}O$	0.9	0.075 (7.5%)	0.025 (2.5%)	Dual	x = 0.25
$Ni_{0.9}Cu_{0.05}Zn_{0.05}O$	0.9	0.05 (5%)	0.05 (5%)	Dual	x = 0.5
$Ni_{0.9}Cu_{0.025}Zn_{0.075}O$	0.9	0.025 (2.5%)	0.075 (7.5%)	Dual	x = 0.75
$Ni_{0.9}Zn_{0.1}O$	0.9	- (0%)	0.1 (10%)	Single	x = 1

3 Results and discussion

3.1 X-ray diffraction (XRD)

Figure 1 shows three distinct pattern planes (111), (200), and (220) of the NiO phase, confirming that the NiO form in cubic structure is consistent with the standard card no. (JCPDS card No. 44-1159). The XRD patterns show pure NiO, single and dual doped NiO nanostructures. This means that dual doping does not change the structure of the NiO nanostructures. The XRD patterns of the prepared samples are calculated according to the following equations [14-16] in Table 2:

$$\frac{1}{d^2} = \frac{(h^2+k^2+l^2)}{a^2} \quad (1)$$

$$D = \frac{k\lambda}{\beta \cos\theta} \quad (2)$$

$$\varepsilon = \frac{\beta_{hkl}}{4\tan\theta} \quad (3)$$

Where d_{hkl} is the interplanar space and (h, k and l) are Miller indices. β is the full width at half maximum (FWHM) of the diffraction peak (200), (λ) is the wavelength of X-ray (λ = 0.154nm) and (θ) is the half angle Bragg diffraction. The low intensity of the XRD patterns for undoped and doped NiO nanostructures (Figure 1) indicates that the samples have low crystallinity due to the nano range of the crystallite size of the prepared samples. Figure 1 shows the XRD patterns of copper and zinc dual doped nickel oxide nanostructures ($Ni_{0.9}(Cu_{1-x}Zn_x)_{0.1}O$) at x= 0, 0.25, 0.5, 0.75 and 1. When x= 0 ($Ni_{0.9}Cu_{0.1}O$), 2θ value of (200) crystal face that showed shifting of diffraction peaks to the lower angle from $43.192^{\circ}$for pure NiO to 43.07° for $Ni_{0.9}Cu_{0.1}O$ sample is predicted as a result of increase lattice constants [14]. Full width at half maximumat β (FWHM) at plane (200) also increase from 0.898° for pure to 1.212° for $Ni_{0.9}Cu_{0.1}O$. The increase in β is due to expansion of the crystal structure as the slightly larger ionic radius of Cu^{2+}(0.73A°) substituted that of Ni^{2+}(0.69A°) in NiO cubic structure [14]. The crystallite size decrease from 9.52 nm for pure NiO to 7.05 nm for $Ni_{0.9}Cu_{0.1}O$ this reduction in the crystallite size for the doped nanoparticles could be attributed to the internal microstructural strain and disorder introduced in the NiO lattice due to incorporation of the Cu ion, this result was in good agreement that published in this literature [11].

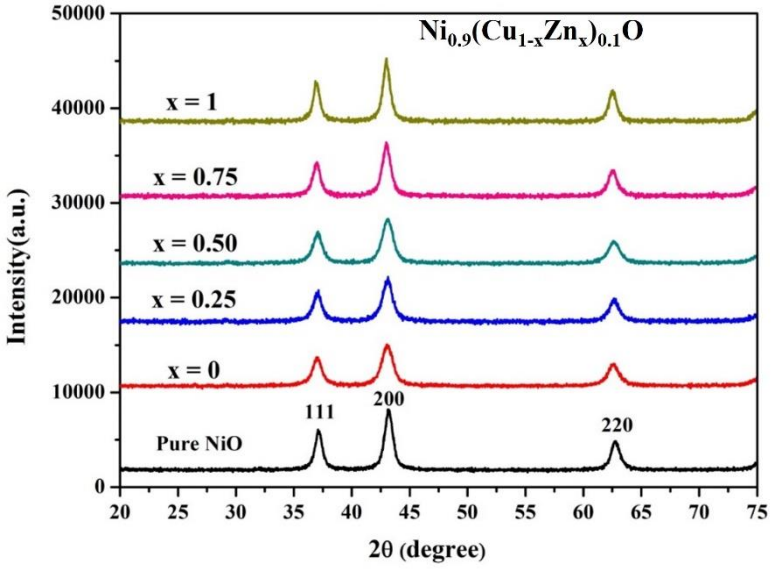

Figure 1. XRD patterns of undoped and doped NiO nanostructures.

For dual doped sample at x = 0.25 ($\mathbf{Ni_{0.9}Cu_{0.075}Zn_{0.025}O}$), **2θ** value of (200) diffraction also shifting to the lower angle by 0.102 due to both dual $\mathbf{Cu^{2+}}$(0.073 nm) and $\mathbf{Zn^{2+}}$(0.074 nm) dopants have larger ionic radii than $\mathbf{Ni^{2+}}$ ions (0.069 nm) [15]. ***β*(FWHM)** ($\mathbf{1.122}^{\circ}$) stilled higher than the pure NiO sample which confirm the substitution of $\mathbf{Ni^{2+}}$ ions

by both $\mathbf{Cu^{2+}}$and $\mathbf{Zn^{2+}}$ ions. The shifting to the lower angle were observed for the other dual samples (x =0.5 and 0.75) as listed in Table 2 due to the same reason mentioned above. But at ($\mathbf{Ni_{0.9}Zn_{0.1}O}$) the shifting to the lower angle , the crystallite size of NiO and Zn doped NiO increased from 9.52 to 10.27 nm due to $\mathbf{Zn^{2+}}$ ions have a large ion radius of 0.074 nm compared to the ionic radius of $\mathbf{Ni^{2+}}$ [16]. The discrepancy between the increase and decrease in the values of microstrain caused with increase in the value of x in structural distortion and cell volume narrowing according to the difference of concentrations. Variation in microstrain may be due to the change in microstructure, size and shape of the particles [16]. In Table 2 the lattice parameter ($\mathbf{a_{hkl}}$), microstrain (ε) and crystallite size (D) values are shown.

Table 2: The structural measurements of prepared samples from (200) diffraction.

Samples	2θ [°]	β= FWHM [°]	a_{200} $[\mathrm{A^{\circ}}]$	D_{200} [nm]	ε_{200} $\times 10^{-3}$
Pure NiO	43.192	0.898	4.1876	9.52	9.9
$\mathbf{Ni_{0.9}Cu_{0.1}O}$	43.07	1.212	4.199	7.05	13.4
$\mathbf{Ni_{0.9}Cu_{0.075}Zn_{0.025}O}$	43.09	1.122	4.1972	7.61	12.4
$\mathbf{Ni_{0.9}Cu_{0.05}Zn_{0.05}O}$	43.10	1.180	4.1962	7.23	13.04
$\mathbf{Ni_{0.9}Cu_{0.025}Zn_{0.075}O}$	43.02	0.953	4.2036	8.95	10.55
$\mathbf{Ni_{0.9}Zn_{0.1}O}$	42.997	0.831	4.2056	10.27	9.21

3.2 Optical properties

Absorbance measurements were performed for pure NiO and $\mathbf{Ni_{0.9}(Cu_{1-x}Zn_x)_{0.1}O}$ nanostructures at x= 0, 0.25, 0.5, 0.75 and 1 recorded in the wavelength range from 190 nm to 1100 nm. Fig 2a shows the change of the absorbance spectra as a function of the wavelength. Figure 2a shows the UV–Vis absorption spectra with the absorption peak of pure NiO at about 332 nm while, $\mathbf{Ni_{0.9}(Cu_{1-x}Zn_x)_{0.1}O}$ presente the absorption peaks at the range of (309 – 319 nm) that indicate to blue shift of the absorption peaks . Optical absorption data at x= 0 indicated strong absorption peaks shifted towards blue (to higher wavelength) with respect to the peak of undoped NiO NPs due to quantum confinement effect[10]. The blue shift of the absorption peaks occur because of Burstein–Moss effect, which confirm the quantum confinement effect [11]. In Figure 2b it can observed that the transmittance of pure NiO nanostructure reduces after the incorporation of the single and dual doped NiO nanostructures. The obtained transmittance was found to be about 85% for pure NiO while in the range (75 - 78%) of transmittance for

single and dual doped NiO nanostructures, this range located in the visible light spectra. This results are consistent with the previous studies [10, 11].

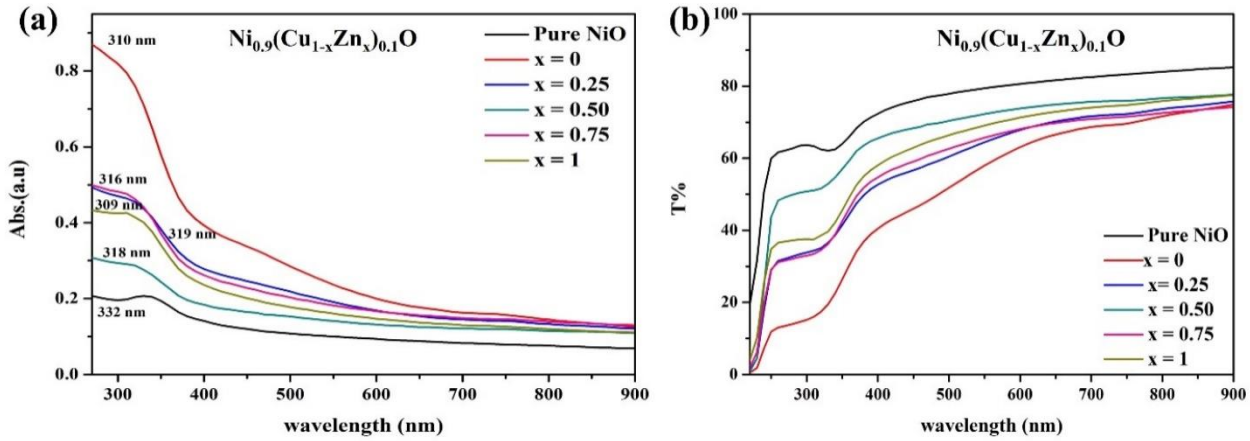

Figure 2. (a) Absorbance and (b) Transmittance spectra of undoped and doped NiO nanostructures.

The absorption coefficient (α) of the prepared samples can be calculated as follows [17]:

$$\boldsymbol{\alpha = 2.303\frac{A}{d}} \qquad (4)$$

Where (d) is the thickness of the sample cell and (A) is the measured absorbance by UV–Visible Spectrophotometer in as plotted in Figure 2a. The optical band gaps of samples have been calculated from Tauc's plot equation [18, 19] an extrapolation of the linear region of the plot $(\boldsymbol{\alpha h\upsilon})^{\boldsymbol{2}}$ versus energy $(\boldsymbol{h\upsilon})$ gives the optical bandgap value $\mathbf{E_g}$:

$$\boldsymbol{(\alpha h\upsilon)^2 = B(h\upsilon - E_g)} \qquad (5)$$

where $(\boldsymbol{h\upsilon})$ is the incident photon energy and (B) is a constant depending on the material. Figure 3a shows Tauc plot for pure NiO and $\mathbf{Ni_{0.9}(Cu_{1-x}Zn_x)_{0.1}O}$ at x= 0, 0.25, 0.5, 0.75 and 1. Bandgap energy of pure NiO is 3 eV which was in good agreement value with results that published by Alshahrie et.al., [20] and Hosny [21]. The single and dual doped NiO samples presents higher $\mathbf{E_g}$ values (3.22 – 3.18 eV) than pure samples as listed in Table 3. The results clearly indicate that the doping increased the band gap which indicated formation of smaller particle size due to quantum confinement effect that agree with Amita et.al., [22]. In general, the charge transfer from the O 2p states to the unoccupied Ni 3d states affected directly by the distortion of the $\mathbf{NiO_6}$ octahedra due to the increasing of dopant content [23]. The dopant occupation of the Ni sites indicates to reduce the nonlocal Zhang-Rice bound state, thus the band gap energy increase. The maximum change in bandgap of NiO were observed for $\mathbf{Ni_{0.9}Cu_{0.1}O}$ (3.22 eV) at x= 0.25.

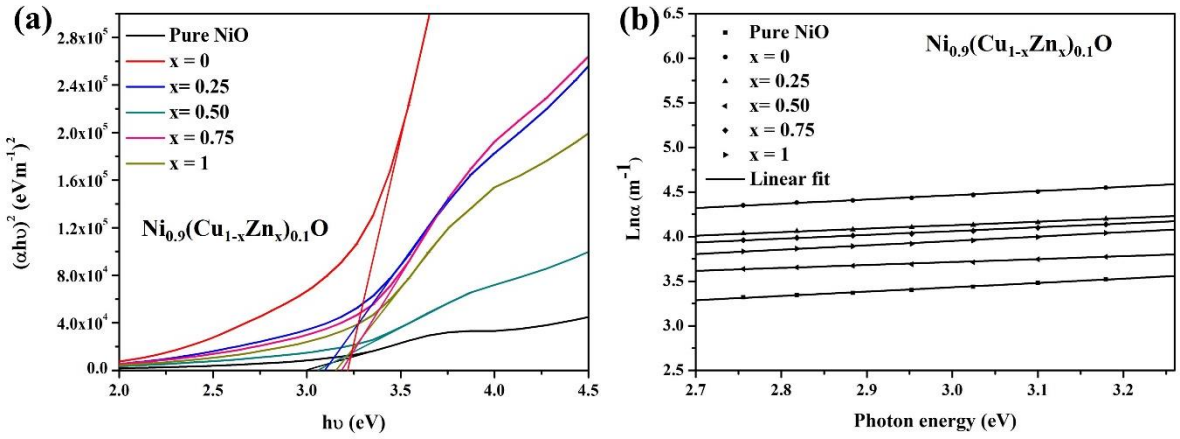

Figure 3. (a) Optical band gap energy (Eg) and inset shows the cut-off values on horizontal axis (photon energy axis). (b) Lnα versus E fitted to the best straight lines for the undoped and doped NiO nanostructures.

Table 3: The optical band gap and Urbach tail energies of prepared samples.

Samples	E_g [eV]	E_u [eV]
Pure NiO	3	2.06
$\mathbf{Ni_{0.9}Cu_{0.1}O}$	3.22	2.10
$\mathbf{Ni_{0.9}Cu_{0.075}Zn_{0.025}O}$	3.1	2.54
$\mathbf{Ni_{0.9}Cu_{0.05}Zn_{0.05}O}$	3.06	3.04
$\mathbf{Ni_{0.9}Cu_{0.025}Zn_{0.075}O}$	3.18	2.34
$\mathbf{Ni_{0.9}Zn_{0.1}O}$	3.16	2.04

The Urbach tail width calculated using equation [24, 25]:

$$\boldsymbol{\alpha = \alpha_0 exp\ (hv/E_u)} \qquad (6)$$

where $\boldsymbol{\alpha_0}$ is characteristic constant depends on materials. The plotting data of on y-axis versus corresponds to the exponential range (Urbach tail range) on x-axis explored a linear relation as shown in Figure 3b. The values were obtained for all prepared samples from the inverse of the slope values of the linear fit and listed in Table 3. Urbach tail energy $\mathbf{E_u}$ values followe the opposite behavior of band gap energy values because of the increase of the disorder and defect states with dopant [12]. The minimum value of $\mathbf{E_u}$ was 2.04 eV at x=1.

The refractive index (n) and absorption index (k) calculated from equation [24]:

$$\boldsymbol{k = \frac{\alpha\lambda}{4\pi}} \qquad (7)$$

$$n=\frac{1+R^{1/2}}{1-R^{1/2}} \quad (8)$$

Figure 4a shows the single and dual doped NiO NPs that indicated the higher refractive index at x= 0 and x= 0.75 respectively. Results presented that Cu dopants increased the refractive index due to higher polarization of Cu atoms in the NiO lattice matrix and in pure NiO sample was the lowest one indicated that NiO host lattice doesn't contain major defects [26]. The real and imaginary parts of the dielectric constant can be calculated from equation [27, 28]:

$$\boldsymbol{\varepsilon = \varepsilon_1 - i\varepsilon_2} \quad (9)$$

$$\varepsilon_1 = n^2 - k^2 \text{ and } \varepsilon_2 = 2nk \quad (10)$$

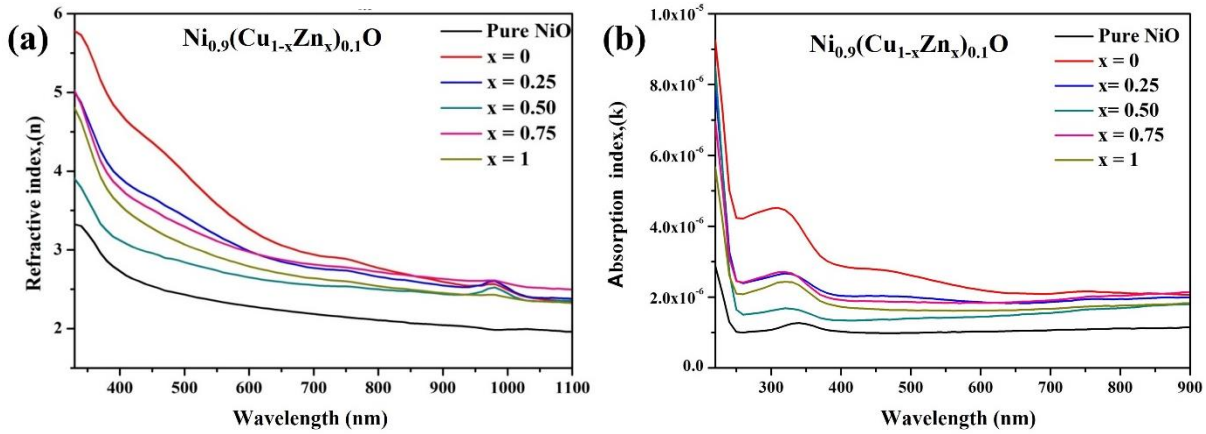

Figure 4. (a) Refractive index (n), and (b) Absorption index (k) of undoped and doped NiO nanostructures as a function of wavelength at different values of x.

The calculated values of $\boldsymbol{\varepsilon_1}$and $\boldsymbol{\varepsilon_2}$ as functions in the photon energy for prepared pure, single and dual doped NiO nanostructures are shown in Figure 5. From Figure 5a shows the calculate value of the real parts of the dielectric constant for samples between 11 s/m and 33.11 s/m in range~$\boldsymbol{3.7}$ **eV**. The single doped NiO at x= 0 (10 wt.% Cu and 0 wt.% Zn) and dual doped NiO at x= 0.75 (2.5 wt.% Cu and 7.5 wt.% Zn) obtained the higher values of dielectric constant. It can be observed that the value of real and the imaginary parts of dielectric increasing with increase doping.

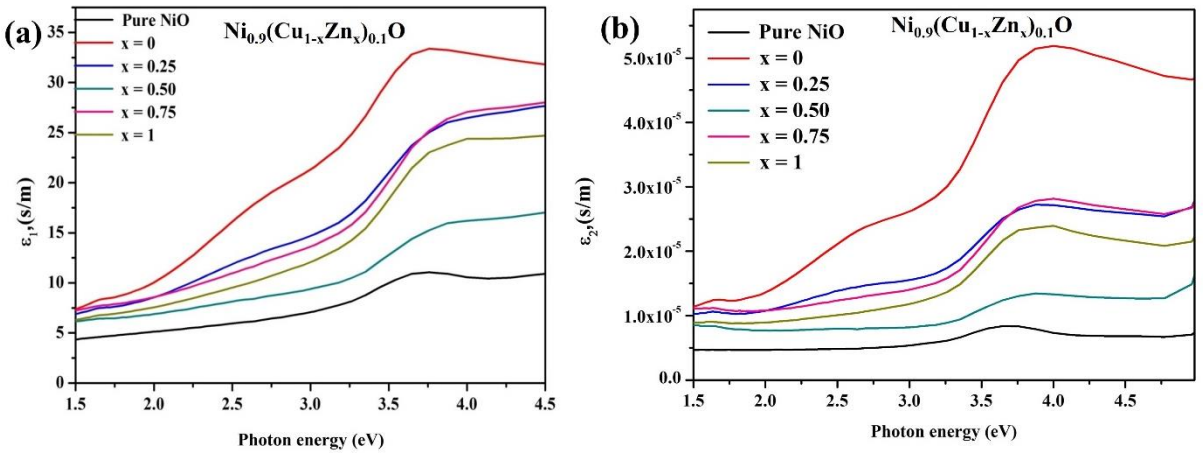

Figure 5. (a) The real ($\boldsymbol{\varepsilon_1}$) and imaginary ($\boldsymbol{\varepsilon_2}$) (b) parts of the dielectric constant on the photon energy for the undoped and doped NiO nanostructures.

Optical conductivity ($\boldsymbol{\sigma_{opt}}$) of the pure and doped NiO nanostructures can be calculated from equation[29]:

$$\boldsymbol{\sigma_{opt}} = \frac{\boldsymbol{\alpha n c}}{\boldsymbol{4\pi}} \qquad (11)$$

whereα, n and c are given by, absorption coefficient, refractive index and speed of light (3×10^8 m/s), respectively. In Figure 6 can observed that the optical conductivity increasing with increase photon energy for all samples. The prepared samples exhibited the maximum of σ_{opt} in range from 2.4×10^{10} to $3.6\times 10^{9}\ s^{-1}$ over ultraviolet region and minimum value in range 1.1×10^{10} to $2.6 \times 10^{9}\ s^{-1}$ over visible light region which approved that these samples preserve good photo response.

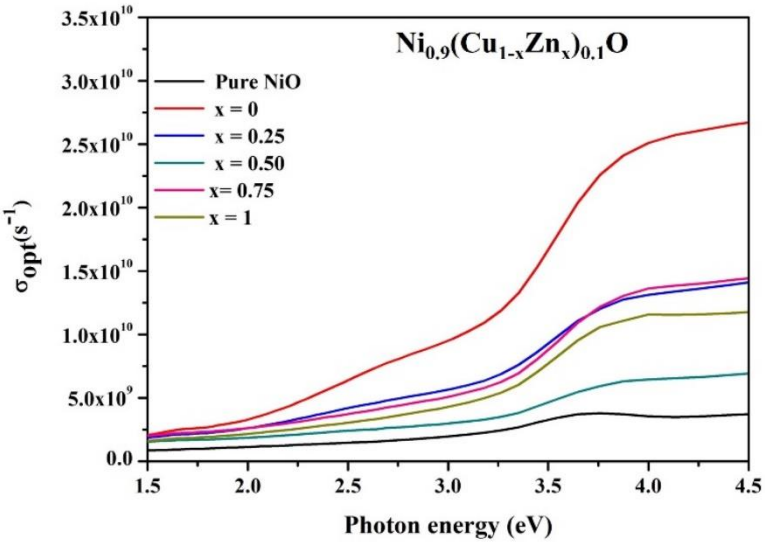

Figure 6. Optical conductivity on the photon energy for the undoped and doped NiO nanostructures.

3.3 DC electrical conductivity (σ_{dc})

Current-voltage measurements are in order to evaluate electrical properties of pure NiO, single and dual doped NiO nanostructures. The resistance (R) is obtaining from the I-V measurements. The DC electrical conductivity values was measured for all prepared samples using the following formula [30]:

$$\boldsymbol{\sigma_{dc}} = \frac{\mathbf{1}}{\mathbf{R}} \times \frac{\mathbf{l}}{\mathbf{A}} \qquad (12)$$

where R is the measured resistance, *A* is the cross-section area and ***l*** is the pellet thickness. σ_{dc} of NiO by I-V measurements is 3.70×10^{-5} S.cm^{-1} this result close from study Biju [31]. The DC electrical conductivity was affected by substitution of $Cu^{2+}$and Zn^{2+} in NiO crystal lattice that decrease from 1.620×10^{-4} S. cm^{-1} to 2.00×10^{-5} S. cm^{-1}. Figure 7 showed DC conductivity (σ_{dc}) and optical band gap energy (E_g) versus x values for pure NiO and$Ni_{0.9}(Cu_{1-x}Zn_x)_{0.1}O$.

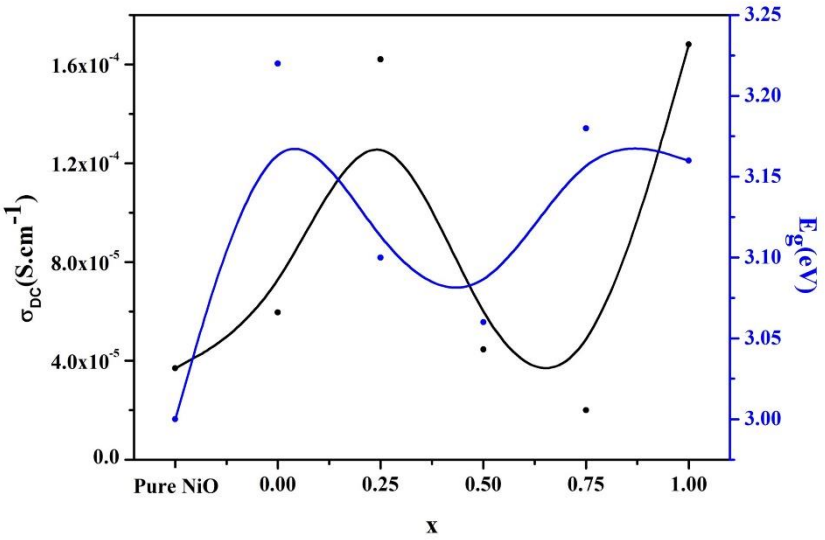

Figure7. DC electrical conductivity σ_{dc} of the NiO samples by I-V measurements versus band gap energy (Eg) as a function of x values. by I-V measurements.

4 Conclusions

Pure NiO, single and dual doped NiO nanostructures with x = 0, 2.5, 5, 7.5, and 10 wt% were successfully prepared by the co-precipitation method and annealed at 350 ℃ for 2 hours. The XRD patterns showed that the average value of crystallite size was between 7.05 and 10.27 nm. The addition of dopants increases the energy gap (E_g) from 3 eV for pure NiO. The maximum change in the band gap of NiO at x = 0.25 due to the occupation of Ni sites by the dopants indicates a decrease in the nonlocal Zhang-Rice bonding state, which increases the band gap energy. Due to the Cu and Zn cations causing substitutional defects in the NiO band gap, the dual doped NiO samples had lower σ_{dc} values than the single doped samples. Dual doped NiO nanostructures will exhibit novel improved properties when the concentration of metal dopants is changed, or these dopants are replaced by others in photoelectronic applications.

References

[1] Bonomo, M. (2018) Synthesis and characterization of NiO nanostructures: a review, *Journal of Nanoparticle Research* **20**: 222.

[2] Sayyadi, K., Gharani, M., Rahdar, A. (2019) The effect of solvent and temperature on the optical and structural properties of the nickel oxide and Cu-doped nickel oxide nanoparticles, *Advances in Nanochemistry* **1**: 34-40.

[3] Yousaf, S., Zulfiqar, S., Shahi, M.N., Warsi, M.F., Al-Khalli, N.F., Aboud, M.F.A., Shakir, I. (2020) Tuning the structural, optical and electrical properties of NiO nanoparticles prepared by wet chemical route, *Ceramics International* **46**: 3750-3758.

[4] Nakate, U.T., Lee, G.H., Ahmad, R., Patil, P., Bhopate, D.P., Hahn, Y., Yu, Y., Suh, E.-k. (2018) Hydrothermal synthesis of p-type nanocrystalline NiO nanoplates for high response and low concentration hydrogen gas sensor application, *Ceramics International* **44**: 15721-15729.

[5] Karthikeyan, M., Kumar, P.V., Ahamed, A.J., Ravikumar, A. (2020) Synthesis of Mg^{2+} doped NiO nanoparticles and their structural and optical properties by Co-precipitation method, *Journal of Advanced Applied Scientific Research-ISSN* **2454**: 3225.

[6] Ponnusamy, P., Agilan, S., Muthukumarasamy, N. (2015) A Simple route synthesis of Cr-doped NiO nanoparticles and their characterisation studies, *Int. J. Chem. Sci* **13**: 683-692.

[7] Mallick, P., Mishra, N. (2012) Evolution of structure, microstructure, electrical and magnetic properties of nickel oxide (NiO) with transition metal ion doping, *American Journal of Materials Science* **2**: 66-71.

[8] Mahmoud, S.A., Shereen, A., Mou'ad, A.T. (2011) Structural and optical dispersion characterisation of sprayed nickel oxide thin films, *Journal of modern Physics* **2**: 1178-1186.

[9] Rani, B.J., Ravi, G., Yuvakkumar, R., Ravichandran, S., Ameen, F., Al-Sabri, A. (2019) Efficient, highly stable Zn-doped NiO nanocluster electrocatalysts for electrochemical water splitting applications, *Journal of Sol-Gel Science and Technology* **89**: 500-510.

[10] Varunkumar, K., Ethiraj, A.S., Kechiantz, A. (2018) Optical absorption and thermal stability study of Cu doped NiO nanoparticles, AIP Conference Proceedings, AIP Publishing LLC, pp. 030174.

[11] Varunkumar, K., Hussain, R., Hegde, G., Ethiraj, A.S. (2017) Effect of calcination temperature on Cu doped NiO nanoparticles prepared via wet-chemical method: Structural, optical and morphological studies, *Materials science in semiconductor processing* **66**: 149-156.

[12] Al Boukhari, J., Zeidan, L., Khalaf, A., Awad, R. (2019) Synthesis, characterization, optical and magnetic properties of pure and Mn, Fe and Zn doped NiO nanoparticles, *Chemical Physics* **516**: 116-124.

[13] GangaReddy, K., Reddy, M.R. (2023) Physical vapour deposition of Zn^{2+} doped NiO nanostructured thin films for enhanced selective and sensitive ammonia sensing, *Materials Science in Semiconductor Processing* **154**: 107198.

[14] Sathishkumar, K., Shanmugam, N., Kannadasan, N., Cholan, S., Viruthagiri, G. (2015) Synthesis and characterization of Cu^{2+} doped NiO electrode for supercapacitor application, *Journal of Sol-Gel Science and Technology* **74**: 621-630.

[15] Lide, D. (2004) CRC Handbook of Chemistry and Physics, 85 ed., CRC Press, Boca Raton, pp. 2661.

[16] Thangamani, C., Pushpanathan, K. (2016) Optical and dielectric behavior of NiO: Zn quantum dots, *J Chem Pharm Res* **8**: 749-757.

[17] Ahmed, A.A.A., Al-Hesni, N.M., Al-Osta, A.H., Al-Salmi, M.L., Manssor, K.A., Saleh, M., Al-Asbahi, B.A., Qaid, S.M., Ghaithan, H.M., Farooq, W. (2021) Influence of single and dual doping (Ag and Co) on the optical properties of CdS quantum dot thin films for solar application, *Optik* **246**: 167824.

[18] Al-Mushki, A.A., Ahmed, A.A.A., Abdulwahab, A., Al-Asbahi, B.A., Abduljalil, J.M., Saad, F.A., Al-Hada, N.M., Qaid, S.M., Ghaithan, H.M. (2022) Structural, optical, and antibacterial characteristics of mixed metal oxide CdO–NiO–Fe_2O_3 nanocomposites prepared using a self-combustion method at different polyvinyl alcohol concentrations, *Applied Physics A* **128**: 279.

[19] Ahmed, A.A.A., Al-Mushki, A.A., Al-Asbahi, B.A., Abdulwahab, A., Abduljalil, J.M., Saad, F.A., Qaid, S.M., Ghaithan, H.M., Farooq, W., Omar, A.-E.H. (2021) Effect of ethylene glycol concentration on the structural and optical properties of multimetal oxide CdO–NiO–Fe_2O_3 nanocomposites for antibacterial activity, *Journal of Physics and Chemistry of Solids* **155**: 110113.

[20] Alshahrie, A., Yahia, I., Alghamdi, A., Al Hassan, P. (2016) Morphological, structural and optical dispersion parameters of Cd-doped NiO nanostructure thin film, *Optik* **127**: 5105-5109.

[21] Hosny, N.M. (2011) Synthesis, characterization and optical band gap of NiO nanoparticles derived from anthranilic acid precursors via a thermal decomposition route, *Polyhedron* **30**: 470-476.

[22] Amita, Deepak, Arun, Rana, P.S. (2019) Synthesis, characterization and sunlight catalytic performance of Cu doped NiO nanoparticles, AIP Conference Proceedings, AIP Publishing LLC, pp. 020035.

[23] Sawatzky, G., Allen, J. (1984) Magnitude and origin of the band gap in NiO, *Physical review letters* **53**: 2339.

[24] Ahmed, A.A.A., Abdulwahab, A., Talib, Z.A., Salah, D., Flaifel, M.H. (2020) Magnetic and optical properties of synthesized ZnO–$ZnFe_2O_4$ nanocomposites via calcined Zn–Fe layered double hydroxide, *Optical Materials* **108**: 110179.

[25] Ahmed, A.A.A., Al-Hussam, A.M., Abdulwahab, A.M., Ahmed, A.N.A.A. (2018) The impact of sodium chloride as dopant on optical and electrical properties of polyvinyl alcohol, *AIMS Materials Science* **5**: 533-542.

[26] Shkir, M., Arif, M., Ganesh, V., Singh, A., Algarni, H., Yahia, I., AlFaify, S. (2020) An effect of Fe on physical properties of nanostructured NiO thin films for nonlinear optoelectronic applications, *Applied Physics A* **126**: 119.

[27] Mandrić Radivojević, V., Rupčić, S., Srnović, M., Benšić, G. (2018) Measuring the dielectric constant of paper using a parallel plate capacitor, *International journal of electrical and computer engineering systems* **9**: 1-10.

[28] Fox, M. (2001) Interband absorption in, *Optical Properties of Solids* 49-75.

[29] Hassanien, A.S., Akl, A.A. (2015) Influence of composition on optical and dispersion parameters of thermally evaporated non-crystalline Cd50S50− xSex thin films, *Journal of Alloys and Compounds* **648**: 280-290.

[30] Popescu, I., Skoufa, Z., Heracleous, E., Lemonidou, A., Marcu, I.-C. (2015) A study by electrical conductivity measurements of the semiconductive and redox properties of Nb-doped NiO catalysts in correlation with the oxidative dehydrogenation of ethane, *Physical Chemistry Chemical Physics* **17**: 8138-8147.

[31] Biju, V., Khadar, M.A. (2001) DC conductivity of consolidated nanoparticles of NiO, *Materials research bulletin* **36**: 21-33.